Dual Epidermal Growth Factor Receptor and Vascular Endothelial Growth Factor Receptor Inhibition with NVP-AEE788 for the Treatment of Aggressive Follicular Thyroid Cancer

Maher N. Younes,[1] Yasemin D. Yazici,[1] Seungwon Kim,[1] Samar A. Jasser,[1] Adel K. El-Naggar,[2] and Jeffrey N. Myers[1,3]

Abstract

Purpose: Patients with radioiodine-resistant follicular thyroid cancer (FTC) have a poor prognosis, if metastasized, with currently available treatment modalities. Epidermal growth factor (EGF) and vascular endothelial growth factor (VEGF) and their receptors (EGFR and VEGFR) have been reported to be overexpressed in FTC and have been implicated in FTC development. We hypothesized that inhibiting the phosphorylation of EGFR and VEGFR by treatment with NVP-AEE788 (AEE788), a novel dual specific EGFR and VEGFR inhibitor, either alone or in combination with paclitaxel, would inhibit the growth of FTC xenografts in an orthotopic nude mouse model.

Experimental Design: To confirm previous reports, EGF and EGFR expression and vascularity were analyzed in human samples of FTC, Hürthle cell carcinoma, and normal thyroid tissues. EGFR expression in four FTC cell lines was measured using Western blotting. The antitumor effect of AEE788 on FTC cells *in vitro* was evaluated using 3-(4,5-dimethylthiazol-2-yl)-2,5-diphenyltetrazolium bromide assays and Western blotting. The effect of AEE788, alone and in combination with paclitaxel, on FTC tumor growth in an orthotopic nude mouse model was also investigated. Immunohistochemical analysis of EGFR and VEGFR signaling status, cell proliferation, apoptosis, and microvessel density was done.

Results: EGF, EGFR, and vascularity were increased in human thyroid tumor samples and EGFR was increased in FTC cells. AEE788 inhibited FTC cell growth *in vitro* and reduced the phosphorylation status of EGFR, VEGFR, and two downstream targets, AKT and mitogen-activated protein kinase, in FTC cells. AEE788 alone and, to a greater extent, AEE788 plus paclitaxel suppressed FTC tumor growth in the thyroids of nude mice.

Conclusion: Dual inhibition of EGFR and VEGFR by AEE788 could represent a novel approach to the treatment of radioiodine-resistant FTC.

Thyroid cancer is the most common endocrine neoplasm in the United States and accounts for ~1% of all new malignant tumors (1). Follicular thyroid carcinoma (FTC), a well-differentiated form of thyroid cancer, accounts for up to one third of thyroid cancer cases (2).

With standard treatment, including surgical removal of the thyroid and regional metastases followed by radioactive iodine ablation, overall survival rates for FTC exceed 90% (3). Basic treatment principles for differentiated thyroid cancer are well established: initial management includes surgical removal of the thyroid gland and regional metastases, followed by postoperative ablation using radioactive iodine (4). Despite the widespread use of multimodality treatment, survival rates have not improved much in the past few decades (5, 6). However, over time, a subset of thyroid cancers display a reduced ability to uptake iodine, produce thyroglobulin, and/or express the TSH receptor, thereby becoming difficult to monitor and less responsive to radioactive iodine therapy (7). Unfortunately, these tumors often also fail to respond to alternative treatment with external-beam radiation therapy or conventional systemic chemotherapy (8). Thus, patients with radioiodine-resistant FTC have a poor prognosis. Novel forms of therapy are needed for these patients.

The epidermal growth factor (EGF) and its receptor (EGFR) have been reported to be overexpressed in thyroid carcinomas in comparison with normal thyroid tissue (9). In addition, the degree of EGFR expression has been shown to be a prognostic factor in thyroid cancer (10). Moreover, it has been suggested that EGF may play an important role in thyroid tumor development (11). EGF stimulates the growth, proliferation,

Authors' Affiliations: Departments of [1]Head and Neck Surgery, [2]Pathology, and [3]Cancer Biology, The University of Texas M.D. Anderson Cancer Center, Houston, Texas

Received 3/30/06; accepted 3/30/06.

Grant support: M.D. Anderson PANTHEON, National Cancer Institute Specialized Program of Research Excellence grant P50CA097007, and NIH Cancer Center Support grant CA016672.

The costs of publication of this article were defrayed in part by the payment of page charges. This article must therefore be hereby marked *advertisement* in accordance with 18 U.S.C. Section 1734 solely to indicate this fact.

Requests for reprints: Jeffrey N. Myers, Department of Head and Neck Surgery, Unit 441, The University of Texas M.D. Anderson Cancer Center, 1515 Holcombe Boulevard, Houston, TX 77030-4009. Phone: 713-792-6920; Fax: 713-794-4662; E-mail: jmyers@mdanderson.org.

doi:10.1158/1078-0432.CCR-06-0793

and invasion of FTC cells, and blockade of EGFR signaling decreases the growth and invasion of FTC cells in culture (12).

Angiogenesis plays a pivotal role in the pathogenesis and growth of differentiated thyroid cancer. The relevance of tumor angiogenesis in thyroid tumors is shown by significant correlations between microvessel density and increasing size of the primary tumor, intrathyroid tumor spread, and disease-free survival (13, 14). One of the most well-studied proangiogenic factors in thyroid tumors is the vascular endothelial growth factor (VEGF; ref. 15). VEGF production is higher in FTC than in normal or benign thyroid tissues (16) and several animal and clinical studies suggest that VEGF expression by thyroid cancer cells is associated with a more aggressive phenotype (17, 18). In addition, down-modulation of VEGF production or inhibition of VEGF receptor (VEGFR) activation has led to reduced growth of FTC xenografts (17, 19).

These data suggest that dual blockade of EGFR and VEGFR signaling could represent an alternative approach to the treatment of locally aggressive and radioiodine-resistant FTC. NVP-AEE788 (AEE788), a member of the 7*H*-pyrrolo[2,3] class of pyrimidines, is a novel orally available dual specific inhibitor of EGFR and VEGFR (20). Its efficacy against a variety of tumors (squamous cell carcinoma of the skin and oral cavity, anaplastic thyroid cancer, prostate cancer, and pancreas cancer) has been verified in preclinical animal models (21–24). We previously established that AEE788 in combination with paclitaxel led to significant reduction in FTC-induced bone metastatic lesions in nude mice (25).

We hypothesized that inhibiting the phosphorylation of EGFR and VEGFR2 with AEE788, either alone or in combination with paclitaxel, would inhibit the growth of FTC xenografts in an orthotopic nude mouse model. In the present study, we investigate whether EGF and EGFR and tumor vascularity are truly increased in human FTC specimens when compared with normal thyroid tissue. We evaluated the expression of EGFR and Her2/neu and the effect of AEE788 on the growth of four FTC cell lines. We also analyzed the effect of AEE788 on the phosphorylation status of EGFR, VEGFR, and two downstream targets involved in survival and proliferation, AKT and mitogen-activated protein kinase (MAPK), respectively. We tested whether the administration of AEE788, alone or in combination with paclitaxel, to athymic nude mice, harboring human FTC tumor cells injected in their thyroid glands, would block the EGFR and VEGF signaling pathways and inhibit tumor progression and growth.

Materials and Methods

Measurement of EGF, EGFR, and vascularity in human thyroid cancer specimens and normal thyroid tissue. To confirm whether EGF and EGFR expression and vascularity are truly increased in human FTC specimens compared with normal tissue, we did immunohistochemical evaluations of surgical specimens in a human tissue microarray. The microarray contained 6 samples of normal thyroid tissue, 18 samples of FTC, and 6 samples of Hürthle cell carcinoma, a more aggressive variant of FTC. The array was obtained from Dr. Adel El-Naggar (Department of Pathology, M.D. Anderson Cancer Center). To measure vascularity, we measured CD34, a transmembrane glycoprotein constitutively expressed on endothelial cells and hematopoietic stem cells.

FTC cell lines and culture conditions. The cell lines used in this study were the radioiodine-resistant FTC cell lines WRO (26), FTC133, FTC236, and FTC238 (27). All cell lines were maintained as monolayer cultures in DMEM supplemented with 10% fetal bovine serum (FBS), nonessential amino acids, sodium pyruvate, L-glutamine, vitamin, and penicillin-streptomycin (all from Life Technologies, Inc., Grand Island, NY). Cell cultures were maintained and incubated as previously described (25).

Measurement of expression of EGFR and Her2/neu in FTC cell lines. We used Western blotting to measure the expression of EGFR (also known as Her1) and Her2/neu (a receptor with extensive homology to EGFR) in the four FTC cell lines and in normal thyroid tissue. Cell lysates were obtained and subjected to Western blotting as previously described in the following sections (22).

Drugs. AEE788 (20) was generously provided by Novartis Pharma AG (Basel, Switzerland). For use *in vitro*, AEE788 was dissolved in DMSO (Sigma-Aldrich Corp., St. Louis, MO) to a concentration of 20 mmol/L and further diluted to an appropriate final concentration in DMEM. The concentration of DMSO in the final solution did not exceed 0.1% (v/v). For oral gavage, AEE788 was dissolved in 90% polyethylene glycol 300 plus 10% 1-methyl-2-pyrrolidinone to a concentration of 6.25 mg/mL and given to mice at a concentration of 50 mg/kg thrice weekly (20).

Paclitaxel (Mead Johnson, Princeton, NJ) was diluted in HBSS to a final concentration of 1 mg/mL and given by i.p. injection at 200 μg once weekly, a dosing regimen that was chosen on the basis of previous studies at our institution (28).

Measurement of effects of AEE788 on proliferation of FTC cells. To test our hypothesis that FTC cell lines would be susceptible to targeted therapy with the dual EGFR and VEGFR inhibitor AEE788, we first evaluated the antiproliferative activity of AEE788 against WRO and FTC133 cells in culture using the tetrazolium-based colorimetric [3-(4,5-dimethylthiazol-2-yl)-2,5-diphenyltetrazolium bromide (MTT)] assay. Specifically, 4×10^3 WRO cells or 1×10^3 FTC133, FTC236, or FTC238 cells were plated for 24 hours into a 96-well plate. Cells were washed twice using DMEM with 2% FBS medium and incubated for 72 hours with AEE788. The cells were then incubated for 2 hours in medium containing MTT and lysed using DMSO. The conversion of MTT to formazan by metabolically viable cells was monitored with a 96-well microtiter plate reader at an absorbance of 570 nm (Dynatech, Inc., Chantilly, VA).

***Measurement of effects of AEE788 on EGF-mediated growth and survival signaling pathways in FTC cells* in vitro.** We next determined whether AEE788 could inhibit EGF-mediated growth and survival signaling pathways in FTC cells growing in culture. We used the more sensitive WRO cell line and the less sensitive FTC133 cell line to study the ability of AEE788 to inhibit EGF-induced tyrosine phosphorylation of EGFR, VEGFR, and two downstream targets of these signaling receptors, MAPK and AKT. Under serum-free conditions, cells showed a low level of autophosphorylation that was enhanced after exposure to recombinant human EGF for 15 minutes. Cells were plated onto a six-well plate at a concentration of 4×10^5 per well and incubated in DMEM with 10% FBS medium overnight. The next day, the cells were washed and incubated with serum-free medium for 24 hours. The study wells were treated with AEE788 at a concentration ranging from 0 to 5 μmol/L whereas the control wells were treated with DMSO for 1 hour. Then, cells were activated with recombinant human EGF (25 ng/mL) for 15 minutes, washed with PBS, and scraped with lysis buffer as previously described (22). The proteins (70 μg) were resolved on 10% SDS-polyacrylamide gels and transferred onto 0.45-μm polyvinylidene difluoride membranes. The membranes were probed overnight with the desired primary antibodies. After incubation with appropriate secondary antibodies, signals were visualized using the SuperSignal West Pico chemiluminescent system from Pierce (Rockford, IL).

Establishment of an orthotopic nude mouse model of FTC. Eight- to 12-week-old male athymic nude mice were purchased from the National Cancer Institute (Bethesda, MD) and housed in a specific pathogen-free facility. The animals were fed irradiated mouse chow and autoclaved reverse osmosis–treated water. All of the animal procedures

were done in accordance with a protocol approved by the Institutional Animal Care and Use Committee.

To establish an orthotopic model for FTC, we adopted an established orthotopic nude mouse model for anaplastic thyroid cancer (29). First, mice were anesthetized with i.p. injection of sodium pentobarbital (50 mg/kg). WRO cells (5×10^5) were suspended DMEM with 0% FBS at a final dilution of $1 \times 10^5/\mu L$. Five microliters (5×10^5 cells) of that suspension were injected into the thyroid glands of each mouse. In brief, a midline cervical incision was made. Afterwards, the underlying submandibular glands were retracted laterally and the central compartment of the neck was visualized. Direct injection of the right thyroid gland was then done using a 25-μL Hamilton syringe (Hamilton Company, Reno, NV) and a 30-gauge hypodermic needle. The submandibular glands were returned to the original location and the skin was closed in a single layer with the use of staples.

Drug treatment of nude mice with human FTC cells injected into their thyroid glands. Five days after intrathyroidal injection of WRO cells, nude mice were randomly divided into four groups of 13 mice each. The control group received the vehicle solution (90% polyethylene glycol 300 plus 10% 1-methyl-2-pyrrolidinone) orally thrice weekly and HBSS by i.p. injection once weekly. The paclitaxel group received 200 μg paclitaxel by i.p. injection once weekly. The AEE788 group received 50 mg/kg AEE788 orally thrice weekly. The AEE788 plus paclitaxel group received 50 mg/kg AEE788 orally thrice weekly and 200 μg paclitaxel by i.p. injection once weekly. All mice were treated for 4 weeks.

Tumor harvest and tissue preparation. The nude mice were treated for 4 weeks and weighed twice per week. At the end of the 4-week treatment period, the mice were asphyxiated using carbon dioxide, and necropsy was done. The cervical lymph nodes and the lungs were removed during the necropsy, sectioned, stained with H&E, and examined for the presence of metastasis. At the time of necropsy, tumor volume was calculated using the formula $(A)(B^2)\pi/6$, where A was the length of the longest aspect of the tumor and B was the length of the tumor perpendicular to A. For immunohistochemical and routine H&E staining, one part of the tumor was fixed in formalin and embedded in paraffin. Another part was embedded in optimal cutting temperature compound (Miles, Inc., Elkhart, IN), rapidly frozen in liquid nitrogen, and stored at −80°C.

Immunohistochemical analysis of markers of vascularization, survival, proliferation, and apoptosis in orthotopic FTC tumors in nude mice. To examine the activity of AEE788, tumor specimens were processed for routine histologic and immunohistochemical analyses for markers of vascularization, survival, proliferation, and apoptosis. *In vivo* cell proliferation and apoptosis were evaluated using anti–proliferating cell nuclear antigen (PCNA) antibodies and terminal deoxynucleotidyl transferase–mediated dUTP nick end labeling (TUNEL), respectively. Paraffin-embedded tissues were used for identification of PCNA, EGF, EGFR, VEGF, VEGFR2, and CD31. The sections were dried overnight, deparaffinized in xylene, and dehydrated in a graded series of alcohol followed by rehydration in PBS. Sections analyzed for PCNA and VEGFR2 were microwaved for 5 minutes for antigen retrieval whereas sections analyzed for VEGF and EGFR were incubated for 20 minutes with pepsin at 37°C for antigen retrieval as previously described (25). Frozen tissues were used for identification of CD31, activated EGFR, activated VEGFR2, activated MAPK, activated AKT, and TUNEL. The tissues were sectioned, mounted, and air-dried for 30 minutes. Frozen sections were fixed in cold acetone (5 minutes), 1:1 acetone/chloroform (v/v; 5 minutes), and acetone (5 minutes) and washed with PBS. Immunohistochemical procedures were done as previously described (28). Control samples exposed to the secondary antibody alone showed no specific staining.

Immunofluorescent double staining for CD31 plus activated EGFR, CD31 plus activated VEGFR2, and CD31 plus activated AKT. To study the proposed antiangiogenic effect of AEE788 and its potential ability to inhibit EGFR and VEGFR phosphorylation on tumor-associated endothelial cells, periodate-lysine-paraformaldehyde–fixed frozen tissues were sectioned and prepared as described in the preceding section. Double staining (CD31 plus activated EGFR, CD31 plus activated VEGFR2, and CD31 plus activated AKT) was done as follows: EGFR, VEGFR2, and AKT immunostainings were done after CD31 staining. Samples were incubated with a protein-blocking solution for 5 minutes with a 1:50 dilution of rabbit polyclonal antihuman EGFR antibody (mouse cross-reactive) for 18 hours at 4°C. Secondary goat anti-rabbit antibody conjugated to FITC was added. One hour later, the samples were mounted with Vectashield (Vector Laboratories, Burlingame, CA).

Immunofluorescence microscopy was done using a Nikon Microphot-FX (Nikon, Inc., Garden City, NY) equipped with a HBO 100 mercury lamp and narrow band-pass filters to individually select for green, red, and blue fluorescence (Chroma Technology Corp., Brattleboro, VT). Images were captured using a cooled charged-coupled device Hamamatsu 5810 camera (Hamamatsu Corp., Bridgewater, NJ) and Optimas image analysis software (Media Cybernetics, Silver Spring, MD). Stained sections were examined using a Nikon Microphot-FX microscope equipped with a three-chip charged-coupled device color video camera (model DXC990, Sony Corp., Tokyo, Japan). Photomontages were prepared using Photoshop software (Adobe Systems, Inc., San Jose, CA). Endothelial cells were identified by red fluorescence staining and DNA fragmentation was identified by localized green and yellow fluorescence within the nuclei of apoptotic cells. Photomontages were printed using a Sony digital color printer (model UP-D7000).

Quantification of microvessel density, apoptosis, and cell proliferation. For quantitative analysis of PCNA (proliferation) and CD31 (microvessel density; tumor vascularity), the mean positive area and mean positive intensity were quantified in five random 0.159-mm^2 fields (magnification, ×100) per slide from five slides per study group using the Image-Pro Plus software package (Media Cybernetics). For TUNEL staining quantification (apoptosis), the labeled cells were counted in five random 0.159-mm^2 fields (magnification, ×100) per slide from five slides per study group. The photomontages were prepared using Photoshop software.

Statistical analysis. PCNA, CD31, and TUNEL staining quantification results were compared by independent samples t test. SPSS 12.0 for Windows software (SPSS, Inc., Chicago, IL) was used for statistical analysis.

Results

Expression of EGF and EGFR is elevated in FTC and Hürthle cell carcinoma compared with normal thyroid tissue. To determine the expression level of EGF and EGFR in normal and neoplastic human thyroid tissue, immunohistochemical evaluation was done on tissue arrays of surgical specimens composed of normal thyroid tissue, FTC, and Hürthle cell carcinoma. Immunohistochemical evaluation of these specimens revealed that EGF and EGFR levels were markedly elevated in both FTC and Hürthle cell carcinoma compared with normal thyroid tissue (Fig. 1A and C). Hürthle cell carcinoma, a more aggressive variant of FTC, showed the strongest staining. The mean EGF-positive and EGFR-positive areas were significantly greater in both the FTC and the Hürthle cell tumor samples than in normal thyroid tissue ($P < 0.05$; Fig. 1B and D). Similarly, the mean EGF intensity scores (mean ± SD) for FTC and Hürthle cell carcinoma were $6.36 \pm 2.33 \times 10^8$ and $9.09 \pm 1.50 \times 10^8$ absorbance units (AU), respectively, significantly higher than that for normal thyroid tissue ($1.18 \pm 1.04 \times 10^8$ AU; $P < 0.05$), and the mean EGFR intensity scores for FTC and Hürthle cell carcinoma were $6.61 \pm 2.08 \times 10^8$ and $7.75 \pm 1.35 \times 10^8$ AU, respectively, significantly higher than that for normal thyroid tissue ($1.77 \pm 1 \times 10^8$ AU; $P < 0.05$).

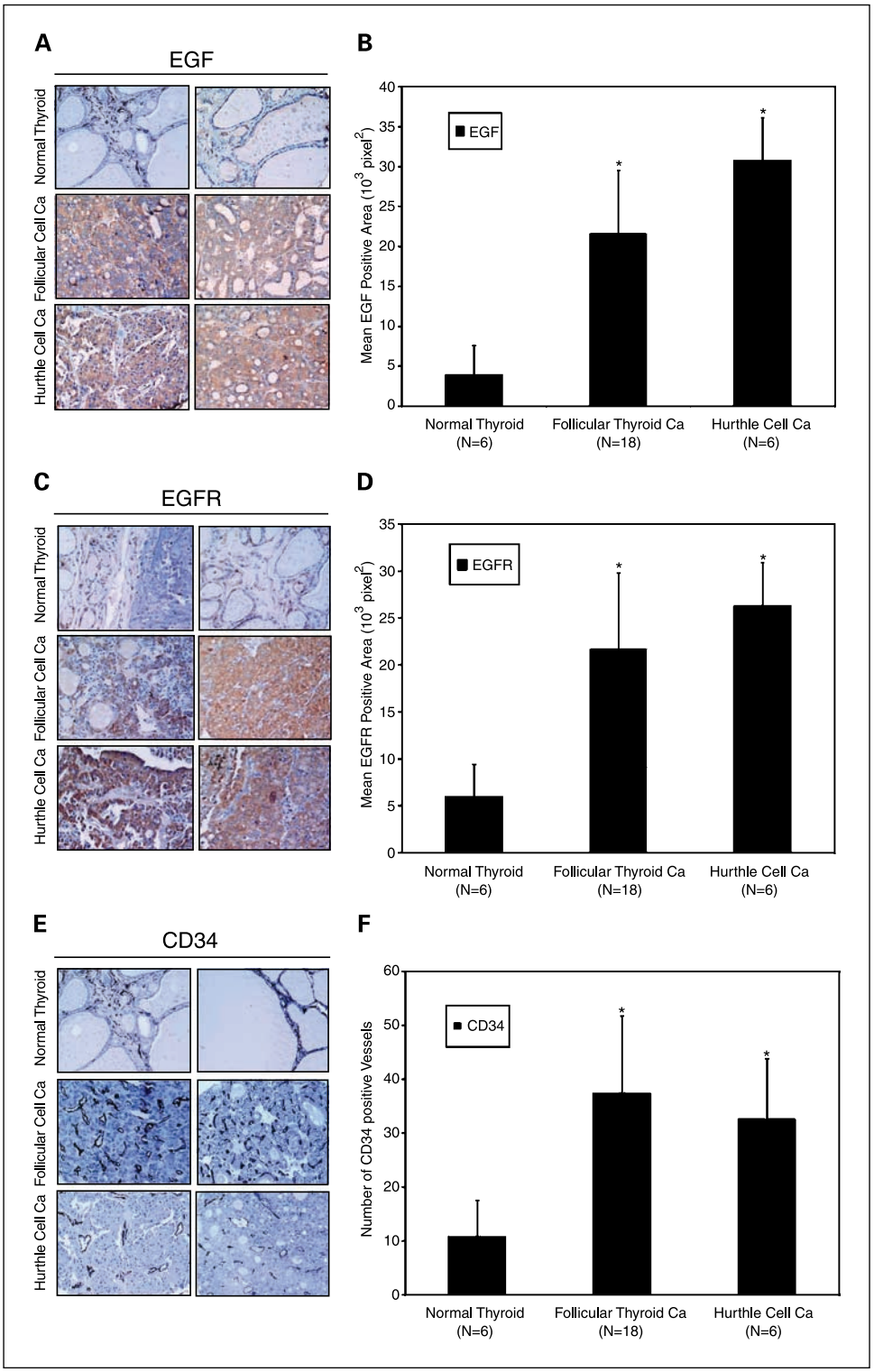

Fig. 1. EGF, EGFR, and CD34 expression in human thyroid cancer and normal thyroid tissue. *A,* EGF was overexpressed in FTC and Hürthle cell carcinoma compared with normal thyroid tissue. *B,* quantitatively, the mean EGF-positive area for normal thyroid tissues (n = 6) was 4.01 $\pm$ 3.52 $\times$ 10^3 pixels^2, significantly lower than the mean EGF-positive area for FTC (n = 18) and Hürthle cell carcinoma (n = 6), which had readings of 21.64 $\pm$ 7.93 $\times$ 10^3 and 30.84 $\pm$ 5.3 $\times$ 10^3 pixels^2, respectively (P < 0.05, compared with normal thyroid). *C,* EGFR was overexpressed in FTC and Hürthle cell carcinoma compared with normal thyroid tissue. *D,* the mean EGFR-positive area for normal thyroid tissue was 6.02 $\pm$ 3.42 $\times$ 10^3 pixels^2, significantly lower than the mean EGFR-positive area for FTC (21.7 $\pm$ 8.11 $\times$ 10^3 pixels^2) for and Hürthle cell carcinoma (26.32 $\pm$ 4.6 $\times$ 10^3 pixels^2). *E,* vascularity, as measured by staining for CD34, was greater in both FTC and Hürthle cell carcinoma than in normal thyroid tissue. *F,* the number of CD34-positive vessels was significantly higher in the tumor specimens (37.48 $\pm$ 14.23 for FTC and 32.64 $\pm$ 11.26 for Hürthle cell carcinoma) than in normal thyroid tissue (10.83 $\pm$ 6.74). Magnification, $\times$100. *, P < 0.05, compared with normal thyroid.

Vascularity is increased in FTC and Hürthle cell carcinoma compared with normal thyroid tissue. The same thyroid tissue array was used to study the vascularity status in normal versus FTC and Hürthle cell carcinoma human slides by immunohistochemical staining for CD34, a transmembrane glycoprotein constitutively expressed on endothelial cells and on hematopoietic stem cells. Immunohistochemically, we found that the number of CD34-positive vessels was significantly higher in FTC and Hürthle cell carcinoma than in normal thyroid tissue (P < 0.05; Fig. 1E and F).

Expression of EGFR and Her2/neu is elevated in human FTC cell lines compared with normal murine thyroid tissue. Western blotting revealed that EGFR protein levels were higher in all four of the FTC cell lines studied—WRO, FTC133, FTC236, and

FTC238—than in normal murine thyroid tissue (Fig. 2A). Her2/neu levels were very low in FTC236 and FTC238 cells, modest in FTC133 cells, and highest in WRO cells (Fig. 2A).

***AEE788 inhibits the proliferation of FTC cells* in vitro.** Taken the elevated levels of EGFR and CD34 in thyroid tumors, we hypothesized that FTC cell line lines would be susceptible to targeted therapy with the dual EGFR and VEGFR inhibitor AEE788. To test this hypothesis, we first evaluated the effect of AEE788 on FTC cells grown in culture using an MTT assay. The growth of the WRO, FTC133, FTC236, and FTC238 cells in DMEM containing 2% FBS was inhibited by AEE788 in a dose-dependent manner. The IC_{50} values were 1.5, 5.1, 3.8, and 2.1 μmol/L, respectively (Fig. 2B).

***AEE788 inhibits the EGF-induced phosphorylation of EGFR, VEGFR2, AKT, and MAPK in FTC cells* in vitro.** Afterwards, we determined whether AEE788 could inhibit EGF-mediated growth and survival signaling pathways in FTC growing in culture. WRO and FTC133 cells were serum starved overnight, treated with increasing concentrations of AEE788 for 1 hour, and then stimulated with EGF for 15 minutes. Western blotting in the WRO cell line revealed complete inhibition of EGFR phosphorylation at an AEE788 concentration of 2 μmol/L and complete inhibition of VEGFR2 phosphorylation at 2 μmol/L (Fig. 2C). The phosphorylated forms of AKT and MAPK were decreased in cells treated with as little as 0.1 μmol/L AEE788. Total levels of EGFR, VEGFR2, AKT, and MAPK were unaltered by AEE788 treatment (Fig. 2C).

Western blotting in the FTC133 cell line, which had the highest IC_{50} for cellular growth, revealed complete inhibition of EGFR phosphorylation at 0.1 μmol/L AEE788 and inhibition of VEGFR2 phosphorylation at 5 μmol/L (Fig. 2D). Similarly, elevated concentrations of AEE788 were required to achieve marked reduction in AKT and MAPK phosphorylation status (Fig. 2D).

AEE788, alone and in combination with paclitaxel, inhibits the growth of FTC in an orthotopic nude mouse model. Because the WRO cell line showed the most sensitivity after treatment with AEE788 in culture (Fig. 2B), it was used to test the effect of AEE788 on FTC growth *in vivo*. WRO cells, when injected into the thyroid glands of athymic nude mice, readily develop into thyroid tumors. Tumor establishment was evident by immunohistochemical analysis 5 days after injection (data not shown).

In the nude mice with established WRO tumors, when paclitaxel was used alone, no reduction in tumor volume compared with control was evident after 4 weeks of treatment (Fig. 3A and B). In contrast, when AEE788 was used alone, a significant reduction in tumor volume was evident after 4 weeks of treatment ($P < 0.01$, compared with control). This reduction was further enhanced when AEE788 and paclitaxel were used in combination ($P < 0.0001$, compared with control; Fig. 3B). There were no detectable cervical or lymph node metastases in any of the groups (data not shown). In summary, there was a 58% and 84% reduction in tumor volume in the AEE788 and combination treatment groups, respectively.

AEE788 blocks EGFR and VEGFR signaling in FTC cells orthotopically implanted in the thyroid glands of nude mice. The level of expression of EGF, VEGF, EGFR, and VEGFR did not vary significantly in tumors from mice treated with placebo, paclitaxel alone, AEE788 alone, or the combination of AEE788 and paclitaxel (Fig. 4A). In contrast, EGFR and VEGFR activation status differed markedly by treatment. When antibodies specific to tyrosine-phosphorylated EGFR and VEGFR were

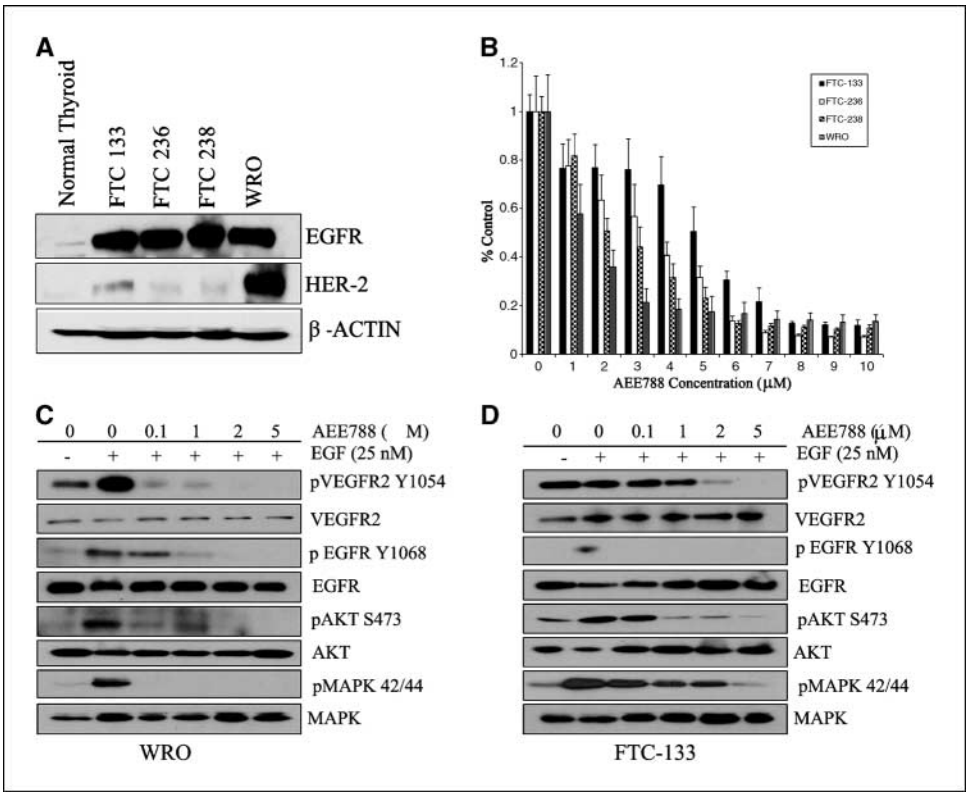

Fig. 2. Expression of EGFR and Her2/neu in thyroid cancer cell lines and dose-dependent inhibition of EGFR and VEGFR signaling in FTC cells after treatment with AEE788. *A,* expression of EGFR (Her1) and Her2/neu receptors in four FTC cell lines and in normal thyroid tissue that was extracted and homogenized. *B,* antiproliferative effects of AEE788 on four FTC cell lines. MTT assays were done to determine the dose-dependent antiproliferative effects of AEE788 on WRO and FTC133, FTC236, and FTC238 cells. Points, average of at least three experiments. *C* and *D,* autophosphorylation of EGFR, VEGFR2, MAPK, and AKT was evaluated in WRO cells (*C*) and FTC133 cells (*D*) growing *in vitro* in serum-free medium and stimulated with recombinant human EGF (25 ng/mL) for 15 minutes in the presence or absence of AEE788. Western blotting was done on protein extracts and the membrane was later probed with antihuman EGFR phosphorylated at Tyr^{1068} (*pEGFR Y1068*), VEGFR2 phosphorylated at Tyr^{1045} (*pVEGFR2 Y1054*), MAPK phosphorylated at Thr^{42}/Thr^{44} (*pMAPK 42/44*), and AKT phosphorylated at Ser^{473} (*pAKT S473*). Total EGFR, VEGFR2, MAPK, and AKT protein levels remained constant. Representative results of three independent experiments.

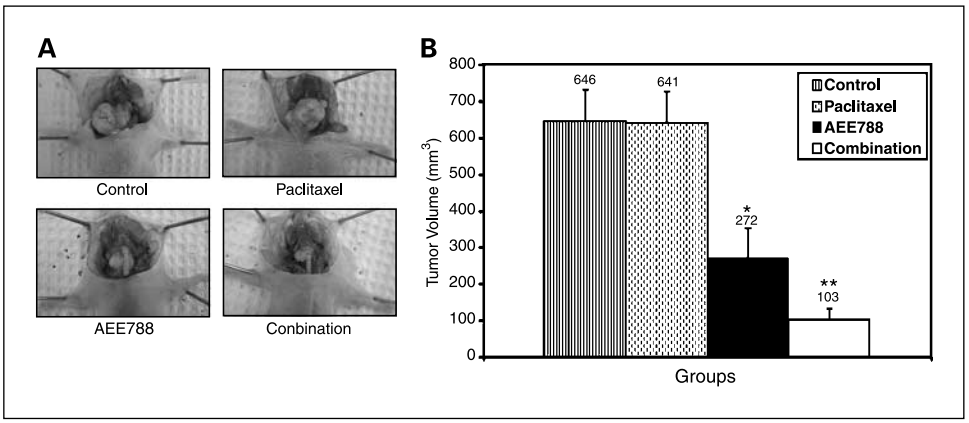

Fig. 3. AEE788 inhibits the growth of FTC xenografts in athymic nude mice. *A,* tumor size after 4 weeks of treatment. WRO cells were injected into the thyroid gland of nude mice. After tumor development, the mice (13 per group) were treated with oral gavage of AEE788 50 mg/kg thrice weekly, paclitaxel given via i.p. injection at 200 μg/injection once weekly, or both AEE788 50 mg/kg thrice weekly and paclitaxel via i.p. injection at 200 μg/injection once weekly. The control mice received HBSS and the AEE788 vehicle, 90% polyethylene glycol 300 + plus 10% 1-methyl-2-pyrrolidinone. *B,* columns, mean tumor volume in mice treated with control, paclitaxel, AEE788 alone, or AEE788 in combination with paclitaxel; bars, SE. *, $P < 0.01$; **, $P < 0.0001$, compared with control tumors.

used, both receptors showed high levels of phosphorylation in the absence of AEE788 treatment and markedly reduced phosphorylation in tumors treated with AEE788 alone or AEE788 plus paclitaxel (Fig. 4B). Similarly, two downstream targets of these signaling receptors, AKT and MAPK, had markedly reduced levels of phosphorylation in tumors treated with AEE788 (Fig. 4B).

AEE788 suppresses angiogenesis by inhibiting EGFR and VEGFR activation on the surface of tumor-associated endothelial cells and by reducing their survival. To determine the effect of AEE788 treatment on tumor vascularity, the microvessel density in tumors from treated mice was determined by staining tumors with CD31. The mean vessel density was highest in the control group and paclitaxel-treated tumors (Table 1). The mean vessel density was significantly decreased ($P < 0.05$) in tumors treated with AEE788 alone or AEE788 plus paclitaxel (Table 1; Fig. 5A). Double staining for CD31 plus activated EGFR and CD31 plus activated VEGFR revealed that only tumors from the mice treated with AEE788 and AEE788 plus paclitaxel had decreased double staining (yellow color) for these markers, a finding consistent with reduced signaling through EGFR and VEGFR in endothelial cells (Fig. 5A). Finally, double staining for CD31 (red staining) plus AKT (green staining) showed that the percentage of endothelial cells (yellow staining) with reduced AKT activation was higher in the tumors of mice treated with AEE788 alone or AEE788 plus paclitaxel than in the controls and mice treated with paclitaxel alone (Fig. 5A).

AEE788 arrests cell proliferation and induces apoptosis in FTC cells growing in the thyroid glands of nude mice. To examine *in vivo* cell proliferation and apoptosis, antibodies were used against PCNA and the TUNEL assay, respectively. As shown in Fig. 5B, PCNA-positive cells were most abundant in the control group and were less abundant in the treated tumors. In addition, TUNEL-positive cells were rarely detected in tumors from control and paclitaxel-treated mice. A progressive increase in the green-fluorescent apoptotic cells was found in tumors from the AEE788 alone and AEE788 plus paclitaxel treatment groups. The percentage of PCNA-positive cells was significantly reduced in the AEE788-treated group and the percentage was lowest in the AEE788 plus paclitaxel group ($P < 0.05$; Table 1). The percentage of dying cells was significantly higher in mice treated with AEE788 or AEE788 plus paclitaxel than in the control group ($P < 0.05$; Table 1).

Table 1. Quantitative immunohistochemical analysis of WRO human FTC tumors growing in thyroid glands of nude mice

Treatment groups*	Tumor cells			Endothelial cells	
	TUNEL†	PCNA		CD31	
		Area‡ (10^3)	Intensity§ (10^8)	Area‡ (10^3)	Intensity§ (10^8)
Control	4.22 ± 1.48	21.81 ± 3.04	3.31 ± 0.33	11.56 ± 3.30	3.40 ± 0.97
Paclitaxel	5.4 ± 3.36	11.89 ± 2.48	3.48 ± 0.75	13.64 ± 5.21	4.15 ± 1.32
AEE788	22.25 ± 9.93	6.08 ± 1.66‖	1.78 ± 0.48‖	5.86 ± 2.34‖	1.72 ± 0.69‖
AEE788 + paclitaxel	34.25 ± 14.26	5.04 ± 1.17‖	1.48 ± 0.34‖	2.74 ± 1.79‖	0.81 ± 0.52‖

*WRO human FTC cells (5×10^5) were injected into the thyroid glands of nude mice. Five days later, groups of mice were randomized into four groups: i.p. injections of paclitaxel (200 μg) alone (once weekly), oral feedings of AEE788 (500 mg/kg) alone (thrice weekly), paclitaxel in combination with AEE788, or placebo (control). All mice were killed after 5 weeks of treatment.

† Median of the ratio of apoptotic endothelial cells to total number of endothelial cells in 10 random 0.011-mm^2 fields at ×400 magnification.

‡ Mean ± SD; mean PCNA- and CD31-positive area as determined from measurement of 10 random 0.159-mm^2 fields at ×100 magnification.

§ Mean ± SD; mean PCNA intensity staining as determined from measurement of 10 random 0.159-mm^2 fields at ×100 magnification.

‖ $P < 0.05$ (Student's *t* test).

Discussion

Our findings indicate that AEE788, alone and in combination with paclitaxel, simultaneously blocks EGFR and VEGFR signaling and significantly reduces FTC tumor volume in nude mice by both direct antitumor and antiangiogenic effects. We found that EGF and EGFR were overexpressed and vascularity was increased in human FTC specimens compared with normal thyroid tissue specimens. We also found that EGFR (Her1) and Her2/neu levels were increased in two of the four human FTC cell lines that we studied. AEE788 reduced cellular proliferation in all four FTC cell lines and inhibited the phosphorylation status of EGFR, VEGFR2, AKT, and MAPK in WRO and FTC133 cells. In an orthotopic nude mouse model of FTC, oral administration of AEE788 alone, thrice per week, reduced final tumor volume by 58%, and AEE788 combined with weekly i.p. injections of paclitaxel reduced final tumor volume by 84%. Immunohistochemical analyses revealed that both AEE788 alone and AEE788 plus paclitaxel blocked EGFR and VEGFR signaling and AKT and MAPK activation. In addition, AEE788

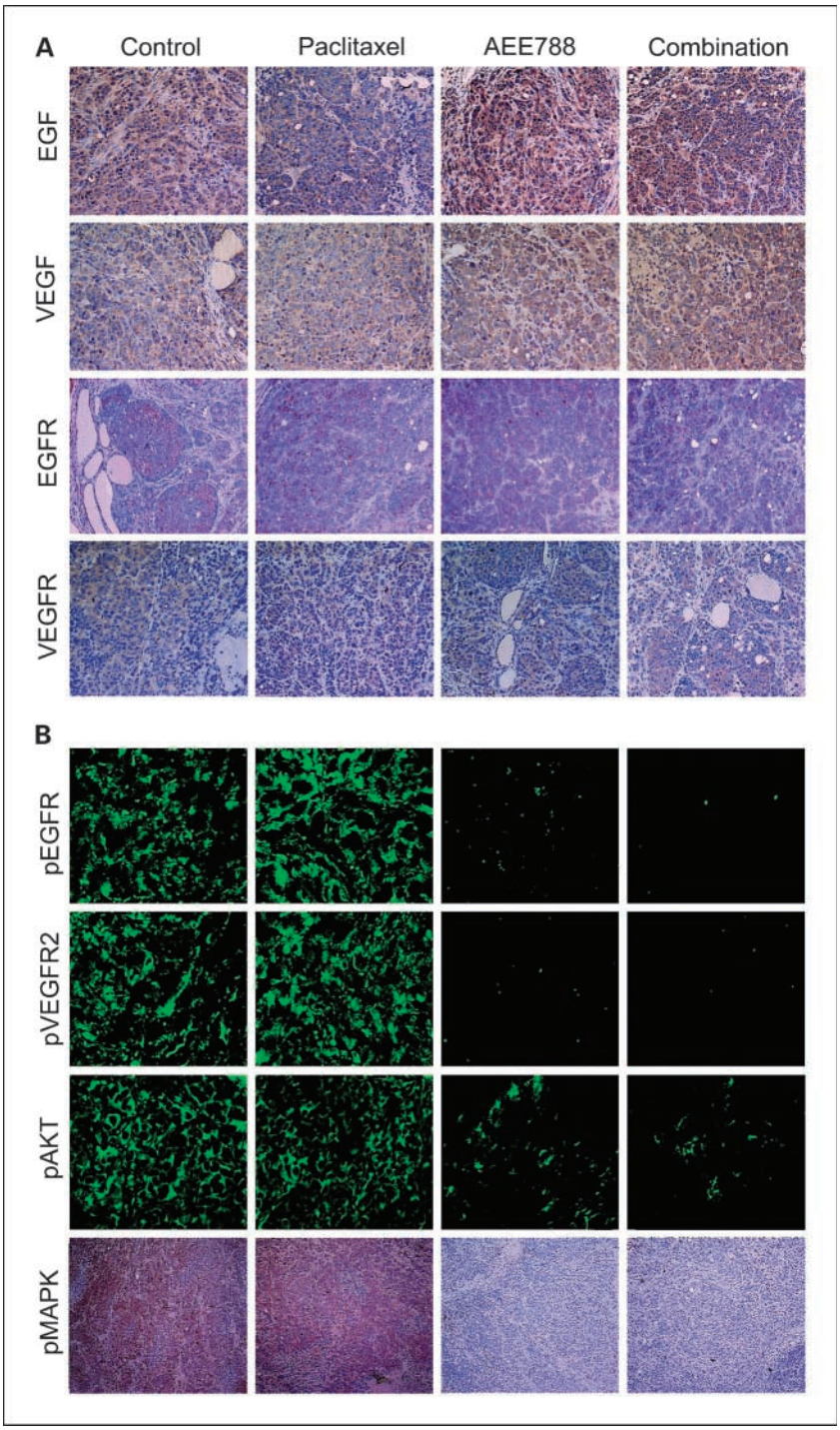

Fig. 4. Dual inhibition of EGFR and VEGFR phosphorylation after treatment with AEE788 alone or in combination with paclitaxel. Tumors derived from WRO FTC cells injected into the thyroids of nude mice were harvested and processed for immunohistochemical analysis after 4 weeks of treatment with HBSS and AEE788 vehicle (control), once-weekly i.p. injection of 200 μg of paclitaxel, thrice-weekly oral administration of AEE788 (50 mg/kg), or paclitaxel plus AEE788. *A,* immunohistochemical analysis using specific anti-EGF, anti-VEGF, anti-EGFR, and anti-VEGFR antibodies showed that WRO tumors from all four treatment groups exhibited similar levels of EGF, VEGF, EGFR, and VEGFR. *B,* specific antibodies to phosphorylated EGFR, phosphorylated VEGFR, phosphorylated AKT, and phosphorylated MAPK showed diminished phosphorylation of all four molecules in tumors from mice treated with AEE788 alone or in combination with paclitaxel compared with tumors from nontreated (control) and paclitaxel-treated mice. Magnification, ×100.

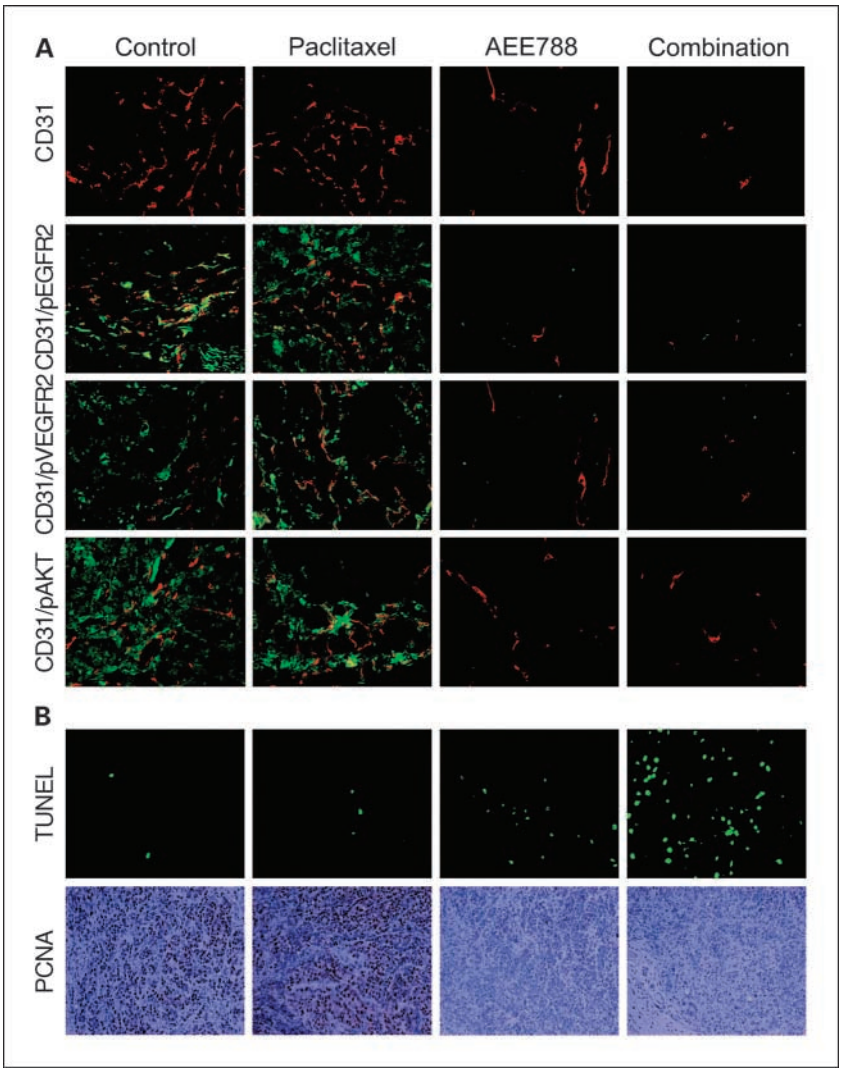

Fig. 5. Suppression of angiogenesis, reduced expression of PCNA, and increased apoptosis in FTC tumors after treatment with AEE788 alone or in combination with paclitaxel. *A,* microvessel density was assessed using antibodies against CD31/platelet endothelial cellular adhesion molecule 1 (*red staining*). In mice treated with AEE788 with or without paclitaxel, CD31/platelet endothelial cellular adhesion molecule 1 reduction was noted. Double staining for CD31 and activated EGFR (*pEGFR*) and for CD31 and activated VEGFR (*pVEGFR2*) was done with CD31 (*red staining*) and with activated EGFR and activated VEGFR (*green staining*). Suppression of the phosphorylation of EGFR and VEGFR on the surface of endothelial cells (marked by the absence of *yellow color*) was detected only in the AEE788-treated tumors with or without paclitaxel administration. Double staining for CD31 (*red*) and activated AKT (*green*) reduced survival in tumor-associated endothelial cells in both AEE788-treated tumor groups (*yellow staining*). Magnification, ×400. *B,* tumors from all four groups were also stained for PCNA and TUNEL. Treatment with AEE788, with or without paclitaxel, reduced expression of PCNA (*brown staining*) and increased apoptosis as marked by TUNEL-positive cells (*green fluorescent staining*). Magnification, ×100.

treatment led to decreased phosphorylation of EGFR and VEGFR on the surface of tumor-associated endothelial cells, leading to reduced survival and significant reduction of microvessel density. As a consequence, tumor cell proliferation was reduced and tumor cell apoptosis was increased.

These results are in close agreement with our previous work (30) and that of others (31) showing that the EGF/EGFR axis is overexpressed in thyroid cancers. Our finding that Her2/neu levels were up-regulated in the WRO and FTC133 cell lines agrees with a previous study that showed that Her2/neu was up-regulated in differentiated thyroid carcinomas (32). Our findings also agree with a previous study showing that EGF and transforming growth factor α stimulated the growth and invasion of FTC133 cells *in vitro* (12), and with another study showing that the blockade of EGFR tyrosine kinase activity by genistein resulted in EGF- and transforming growth factor α–mediated growth and invasion of FTC133 cells (12).

Inhibition of the VEGFR pathway by AEE788 led to a reduction in the number of blood vessels in the tumor mass. In a prior investigation, inhibition of this signaling axis with a specific VEGFR kinase inhibitor, PTK787, alone resulted in a significant reduction in the size of FTC xenografts grown s.c. (19). Our results are similar to those of a number of studies in the literature that targeted VEGFR by overexpressing soluble forms of either VEGFR (sflt-1) or antiangiogenic factors (like endostatin) and showed that this led to reduced growth of FTC xenografts (33, 34).

In our study, oral administration of AEE788, alone or in combination with paclitaxel, significantly decreased microvessel density. Increased vascularity has previously been reported in thyroid tumors (35). Previous studies investigating the numerous antiangiogenic targeted approaches for the treatment of FTC xenografts used the s.c. tumor model. In our study, in which we used orthotopic xenografts, all blood vessels feeding the FTC tumors were, in theory, derived from the thyroid gland. The importance of this difference lies in the fact that endothelial cells from different organs are phenotypically distinct. In our study, only the tumor-associated endothelial cells from the mice treated with AEE788 alone or in combination with paclitaxel had reduced double staining for CD31 plus activated EGFR and CD31 plus activated VEGFR. Bearing in mind that human FTC overexpresses EGF, it is possible that FTC cells stimulate EGFR activation in endothelial cells by a paracrine mechanism through the production of EGF

and possibly transforming growth factor α. Silencing these signaling pathways on endothelial cells makes them more susceptible to taxane-based therapy, as evidenced by their reduced endothelial cell survival (less CD31 plus activated AKT) in response to AEE788 treatment. This in turn deprives tumor cells of their blood supply and triggers more apoptosis in the tumor mass.

In our previous work, we showed that the combination of AEE788 and paclitaxel was effective in reducing the extent and size of FTC-induced bone metastases (25). Thyroid cancer is known for its propensity to metastasize to the regional cervical lymph nodes and lungs. FTC, in particular, has a predilection to metastasize to the lungs. However, in our orthotopic nude mouse model of FTC, we were unable to detect any cervical lymph node or lung metastases. Despite this, AEE788 would still be a suitable candidate for FTC patients suffering from lung metastases because tumor vascularity has been shown to mediate lung metastases in FTC (36).

In addition to inhibiting EGFR and VEGFR phosphorylation, AEE788 also attenuated the activation status of two critical downstream targets involved in proliferation (MAPK) and survival (AKT) while maintaining total levels of these proteins unaltered. This is in agreement with a previous report that showed that whereas total MAPK protein levels remained unaltered, phosphorylated MAPK levels were overexpressed in metastatic thyroid cancer compared with primary tumor samples (37). Inhibiting activated MAPK by U0126, a MAPK/extracellular signal–regulated kinase kinase-1/2 inhibitor, led to reduced cell survival in FTC cells grown in culture (38). In addition, increased levels of activated AKT in FTC have been reported (39, 40). Using a mouse model for spontaneous FTC and subsequent lung metastases, Kim et al. (41) showed that AKT was overexpressed in primary thyroid tumors and that AKT expression was even higher in lung metastases. Our previous work showed that using a specific novel small-molecule inhibitor of AKT, KP372-1, led to the suppression of cellular growth and induction of apoptosis in thyroid cancer cells (42).

Despite the significant reduction in tumor size that we observed in both AEE788-treated groups of mice, no cures were present at the end of 4 weeks. This can be explained by the fact that several other growth factor receptors have been found to be up-regulated in FTC. In fact, our preliminary work found that insulin-like growth factor receptor was up-regulated in the same human tissue array that was used for this study.[4] Intense insulin-like growth factor receptor staining has been linked to more aggressive forms of pediatric thyroid carcinomas (43). In addition to insulin-like growth factor receptor, platelet-derived growth factor receptor has been implicated in the pathogenesis of FTC. A recent report has shown an aberrant autocrine activation of the platelet-derived growth factor α-receptor in FTC cell lines (44). Finally, overexpression of the c-met receptor has been reported in FTCs (45). All these pathways may serve as escape routes allowing FTC to grow and possibly metastasize even when both EGFR and VEGFR are blocked.

In summary, we have shown that simultaneous blockade of EGFR and VEGFR signaling by AEE788 alone or in combination with paclitaxel can significantly reduce FTC tumor volume in nude mice by both direct antitumor and antiangiogenic effects. These data strongly recommend further development of AEE788 for clinical use in the treatment of patients with aggressive and radioiodine-resistant FTC.

Acknowledgments

We thank Stephanie Deming for her editorial review of the manuscript.

[4] Unpublished data.

References

1. Wartofsky L. Epidemiology of thyroid cancer. In: Thyroid cancer: a comprehensive guide to clinical management. Totowa (NJ): Humana Press; 1999.
2. Hundahl SA, Cady B, Cunningham MP, et al. Initial results from a prospective cohort study of 5583 cases of thyroid carcinoma treated in the united states during 1996. U.S. and German Thyroid Cancer Study Group. An American College of Surgeons Commission on Cancer Patient Care Evaluation study. Cancer 2000;89:202–17.
3. Gilliland FD, Hunt WC, Morris DM, Key CR. Prognostic factors for thyroid carcinoma. A population-based study of 15,698 cases from the Surveillance, Epidemiology and End Results (SEER) program 1973-1991. Cancer 1997;79:564–73.
4. Woodrum DT, Gauger PG. Role of 131I in the treatment of well differentiated thyroid cancer. J Surg Oncol 2005;89:114–21.
5. Teppo L, Hakulinen T. Variation in survival of adult patients with thyroid cancer in Europe. Eur J Cancer 1998;34:2248–52.
6. Dinneen SF, Valimaki MJ, Bergstralh EJ, Goellner JR, Gorman CA, Hay ID. Distant metastases in papillary thyroid carcinoma. 100 cases observed at one institution during 5 decades. J Clin Endocrinol Metab 1995;80:2041–5.
7. Braga-Basaria M, Ringel MD. Clinical review 158. Beyond radioiodine: a review of potential new therapeutic approaches for thyroid cancer. J Clin Endocrinol Metab 2003;88:1947–60.
8. Leaf AN, Wolf BC, Kirkwood JM, Haselow RE. Phase II study of etoposide (VP-16) in patients with thyroid cancer with no prior chemotherapy: an Eastern Cooperative Oncology Group Study (E1385). Med Oncol 2000;17:47–51.
9. van der Laan BF, Freeman JL, Asa SL. Expression of growth factors and growth factor receptors in normal and tumorous human thyroid tissues. Thyroid 1995;5:67–73.
10. Akslen LA, Varhaug JE. Oncoproteins and tumor progression in papillary thyroid carcinoma: presence of epidermal growth factor receptor, c-erbB-2 protein, estrogen receptor related protein, p21-ras protein, and proliferation indicators in relation to tumor recurrences and patient survival. Cancer 1995;76:1643–54.
11. Duh QY, Gum ET, Gerend PL, Raper SE, Clark OH. Epidermal growth factor receptors in normal and neoplastic thyroid tissue. Surgery 1985;98:1000–7.
12. Holting T, Siperstein AE, Clark OH, Duh QY. Epidermal growth factor (EGF)- and transforming growth factor α-stimulated invasion and growth of follicular thyroid cancer cells can be blocked by antagonism to the EGF receptor and tyrosine kinase *in vitro*. Eur J Endocrinol 1995;132:229–35.
13. Dhar DK, Kubota H, Kotoh T, et al. Tumor vascularity predicts recurrence in differentiated thyroid carcinoma. Am J Surg 1998;176:442–7.
14. Fenton C, Patel A, Dinauer C, Robie DK, Tuttle RM, Francis GL. The expression of vascular endothelial growth factor and the type 1 vascular endothelial growth factor receptor correlate with the size of papillary thyroid carcinoma in children and young adults. Thyroid 2000;10:349–57.
15. Hanahan D, Folkman J. Patterns and emerging mechanisms of the angiogenic switch during tumorigenesis. Cell 1996;86:353–64.
16. Soh EY, Duh QY, Sobhi SA, et al. Vascular endothelial growth factor expression is higher in differentiated thyroid cancer than in normal or benign thyroid. J Clin Endocrinol Metab 1997;8:3741–7.
17. Belletti B, Ferraro P, Arra C, et al. Modulation of *in vivo* growth of thyroid tumor-derived cell lines by sense and antisense vascular endothelial growth factor gene. Oncogene 1999;18:4860–9.
18. Klein M, Vignaud JM, Hennequin V, et al. Increased expression of the vascular endothelial growth factor is a pejorative prognosis marker in papillary thyroid carcinoma. J Clin Endocrinol Metab 2001;86:656–8.
19. Schoenberger J, Grimm D, Kossmehl P, Infanger M, Kurth E, Eilles C. Effects of PTK787/ZK222584, a tyrosine kinase inhibitor, on the growth of a poorly differentiated thyroid carcinoma: an animal study. Endocrinology 2004;145:1031–8.
20. Traxler P, Allegrini PR, Brandt R, et al. A dual family epidermal growth factor receptor/ErbB2 and vascular endothelial growth factor receptor tyrosine kinase inhibitor with antitumor and antiangiogenic activity. Cancer Res 2004;64:4931–41.
21. Park YW, Younes MN, Jasser SA, et al. AEE788, a dual tyrosine kinase receptor inhibitor, induces endothelial cell apoptosis in human cutaneous squamous cell carcinoma xenografts in nude mice. Clin Cancer Res 2005;11:1963–73.
22. Yigitbasi OG, Younes MN, Doan D, et al. Tumor cell and endothelial cell therapy of oral cancer by dual

tyrosine kinase receptor blockade. Cancer Res 2004; 64:7977–84.

23. Yokoi K, Kim SJ, Thaker P, et al. Induction of apoptosis in tumor-associated endothelial cells and therapy of orthotopic human pancreatic carcinoma in nude mice. Neoplasia 2005;7:696–704.

24. Yazici S, Kim SJ, Busby JE, et al. Dual inhibition of the epidermal growth factor and vascular endothelial growth factor phosphorylation for antivascular therapy of human prostate cancer in the prostate of nude mice. Prostate 2005;65:203–15.

25. Younes MN, Yigitbasi OG, Park YW, et al. Antivascular therapy of human follicular thyroid cancer experimental bone metastasis by blockade of epidermal growth factor receptor and vascular growth factor receptor phosphorylation. Cancer Res 2005; 65:4716–27.

26. Estour B, Van Herle AJ, Juillard GJ, et al. Characterization of a human follicular thyroid carcinoma cell line (UCLA RO 82 W-1). Virchows Arch B Cell Pathol Incl Mol Pathol 1989;57:167–74.

27. Goretzki PE, Frilling A, Simon D, Roeher HD. Growth regulation of normal thyroids and thyroid tumors in man. Recent Results Cancer Res 1990;118: 48–63.

28. Bruns CJ, Solorzano CC, Harbison MT, et al. Blockade of the epidermal growth factor receptor signaling by a novel tyrosine kinase inhibitor leads to apoptosis of endothelial cells and therapy of human pancreatic carcinoma. Cancer Res 2000;60:2926–35.

29. Kim S, Park YW, Schiff BA, et al. An orthotopic model of anaplastic thyroid carcinoma in athymic nude mice. Clin Cancer Res 2005;11:1713–21.

30. Schiff BA, McMurphy AB, Jasser SA, et al. Epidermal growth factor receptor (EGFR) is overexpressed in anaplastic thyroid cancer, and the EGFR inhibitor gefitinib inhibits the growth of anaplastic thyroid cancer. Clin Cancer Res 2004;10: 8594–602.

31. Westermark K, Lundqvist M, Wallin G, et al. EGF-receptors in human normal and pathological thyroid tissue. Histopathology 1996;28:221–7.

32. Haugen DR, Akslen LA, Varhaug JE, Lillehaug JR. Expression of c-erbB-2 protein in papillary thyroid carcinomas. Br J Cancer 1992;65:832–7.

33. Ye C, Feng C, Wang S, et al. sFlt-1 gene therapy of follicular thyroid carcinoma. Endocrinology 2004; 145:817–22.

34. Ye C, Feng C, Wang S, Liu X, Lin Y, Li M. Antiangiogenic and antitumor effects of endostatin on follicular thyroid carcinoma. Endocrinology 2002;143: 3522–8.

35. Ramsden JD. Angiogenesis in the thyroid gland. J Endocrinol 2000;166:475–80.

36. Segal K, Shpitzer T, Feinmesser M, Stern Y, Feinmesser R. Angiogenesis in follicular tumors of the thyroid. J Surg Oncol 1996;63:95–8.

37. Chen KT, Lin JD, Chao TC, et al. Identifying differentially expressed genes associated with metastasis of follicular thyroid cancer by cDNA expression array. Thyroid 2001;11:41–6.

38. Specht MC, Barden CB, Fahey TJ III. p44/p42-MAP kinase expression in papillary thyroid carcinomas. Surgery 2001;130:936–40.

39. Ringel MD, Hayre N, Saito J, et al. Overexpression and overactivation of Akt in thyroid carcinoma. Cancer Res 2001;61:6105–11.

40. Miyakawa M, Tsushima T, Murakami H, Wakai K, Isozaki O, Takano K. Increased expression of phosphorylated p70S6 kinase and Akt in papillary thyroid cancer tissues. Endocr J 2003;50:77–83.

41. Kim CS, Vasko VV, Kato Y, et al. AKT activation promotes metastasis in a mouse model of follicular thyroid carcinoma. Endocrinology 2005;146:4456–63.

42. Mandal M, Kim S, Younes MN, et al. The Akt inhibitor KP372–1 suppresses Akt activity and cell proliferation and induces apoptosis in thyroid cancer cells. Br J Cancer 2005;92:1899–905.

43. Gydee H, O'Neill JT, Patel A, Bauer AJ, Tuttle RM, Francis GL. Differentiated thyroid carcinomas from children and adolescents express IGF-I and the IGF-I receptor (IGF-I-R). Cancers with the most intense IGF-I-R expression may be more aggressive. Pediatr Res 2004;55:709–15.

44. Chen KT, Lin JD, Liou MJ, Weng HF, Chang CA, Chan EC. An aberrant autocrine activation of the platelet-derived growth factor α-receptor in follicular and papillary thyroid carcinoma cell lines. Cancer Lett 2005.

45. Di Renzo MF, Olivero M, Serini G, et al. Overexpression of the c-MET/HGF receptor in human thyroid carcinomas derived from the follicular epithelium. J Endocrinol Invest 1995;18:134–9.

Clinical Cancer Research

Dual Epidermal Growth Factor Receptor and Vascular Endothelial Growth Factor Receptor Inhibition with NVP-AEE788 for the Treatment of Aggressive Follicular Thyroid Cancer

Maher N. Younes, Yasemin D. Yazici, Seungwon Kim, et al.

Clin Cancer Res 2006;12:3425-3434.